Geological Survey of Japan Cruise Report No. 22, p. 85-96, 1992

VI. DEEP-SEA SEDIMENTS IN THE SOUTHERN PART OF THE CENTRAL PACIFIC BASIN (GH82-4 AREA)

Akira Nishimura and Ken Ikehara

Introduction

During the GH82-4 Cruise, areal distribution of sediments and sedimentary history were studied in the south of the Nova-Canton Trough, central Equatorial Pacific (Fig. VI-1) in relation to the genesis of manganese nodules. A small area was selected for small-scale sampling in the eastern margin of the whole survey area (Fig. VI-2). Sampling methods of sediments and manganese nodules are as follows; double spades box corer (15 sites), piston corer (20 sites), and free-fall grab with a small sediment sampler (39 sites).

Box and piston core sites are shown in Tables VI-1 and VI-2 and in Figures VI-1 and VI-2. Sediments collected by a box corer, piston corer, and free-fall grab sampler were treated in the same manner as in previous works (Nishimura, 1984 and 1986). Sediment lithology was classified according to the compositions of sediments determined on smear slides under a microscope.

The framework of sediment classification is shown in Table VI-3. Age estimation of the core sequences are based on preliminary micropaleontologic analysis and a study of remnant magnetism of sediments (Yamazaki, chapter VII of this volume). This chapter describes lithology of sediments and discusses sedimentary history concerning surface sediments and core sequences.

Surface Sediments

The distribution map of surface sediment of the Pacific (Piper *et al.*, 1985) indicates that the surface sediment of the survey area is biosiliceous mud. In more details, Nakao and Mizuno (1982) surveyed the transect from Wake to Tahiti crossing this survey area, and they recognized sedimentary provinces based on sediment lithology. According to them, this survey area is included into *Equatorial siliceous biogenic zone* characterized by abundant occurrence of radiolarians, diatoms, and sponge spicules, which is formed related to an equatorial high productivity zone.

The surface sediments of box cores (Fig. VI-3) and the uppermost sediments of piston cores are brown to dark yellowish brown siliceous clay, which includes a lot of radiolarian and diatom tests. Calcareous biogenic components, such as planktonic foraminifers and calcareous nannoplanktons are lacking or very rare because the survey area is deeper than calcium carbonate compensation depth (CCD). The CCD of this area is estimated to be approximately 5000 m (Berger, 1976; Takayanagi *et al.*,

Keywords: siliceous sediment, microfossil, CCD, turbidite, sedimentation rate, antarctic bottom water, hiatus, Central Pacific Basin, Hakurei-Maru, Nova-Canton Trough

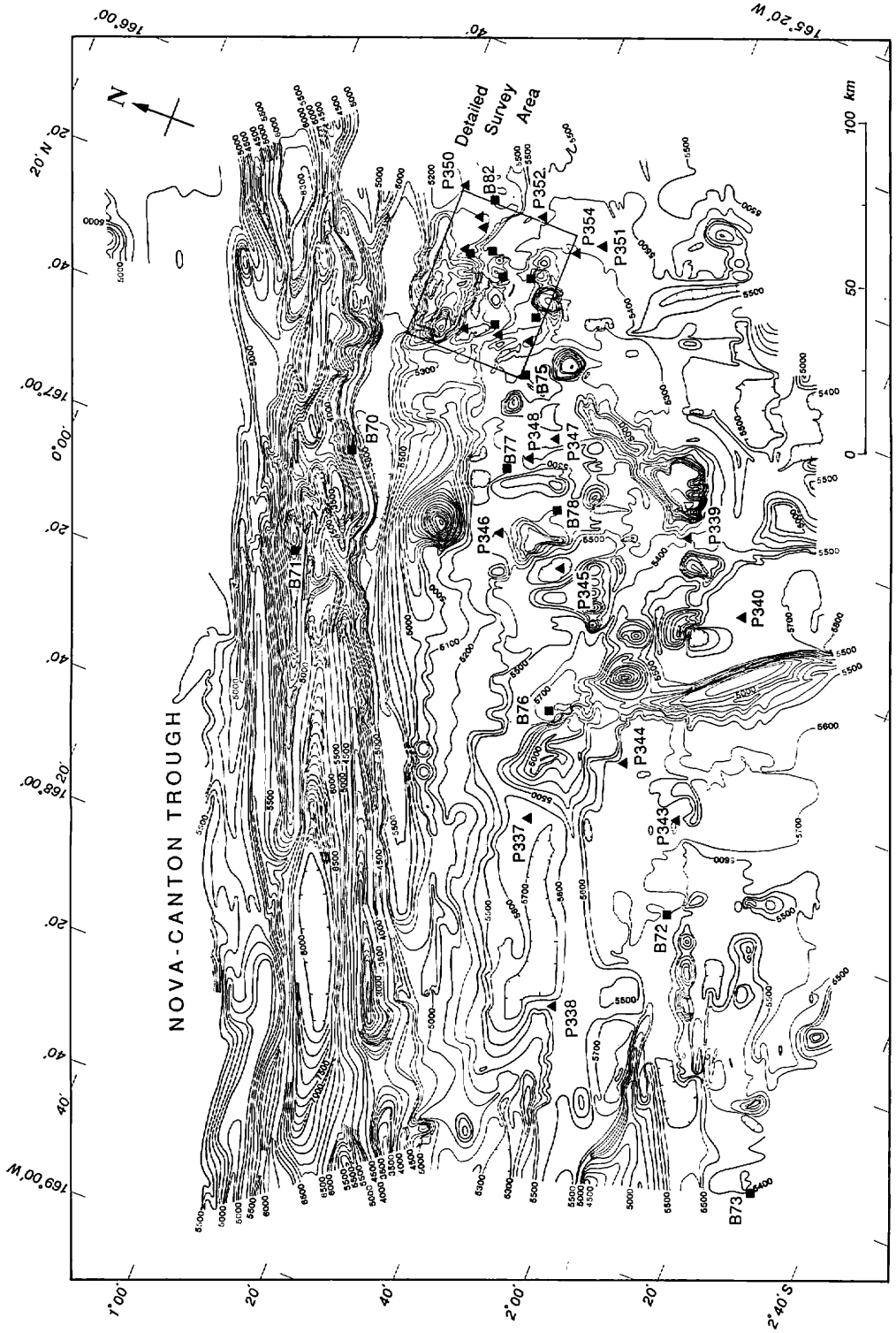

Fig. VI-1 Topography and sampling stations of the GH82-4 area.

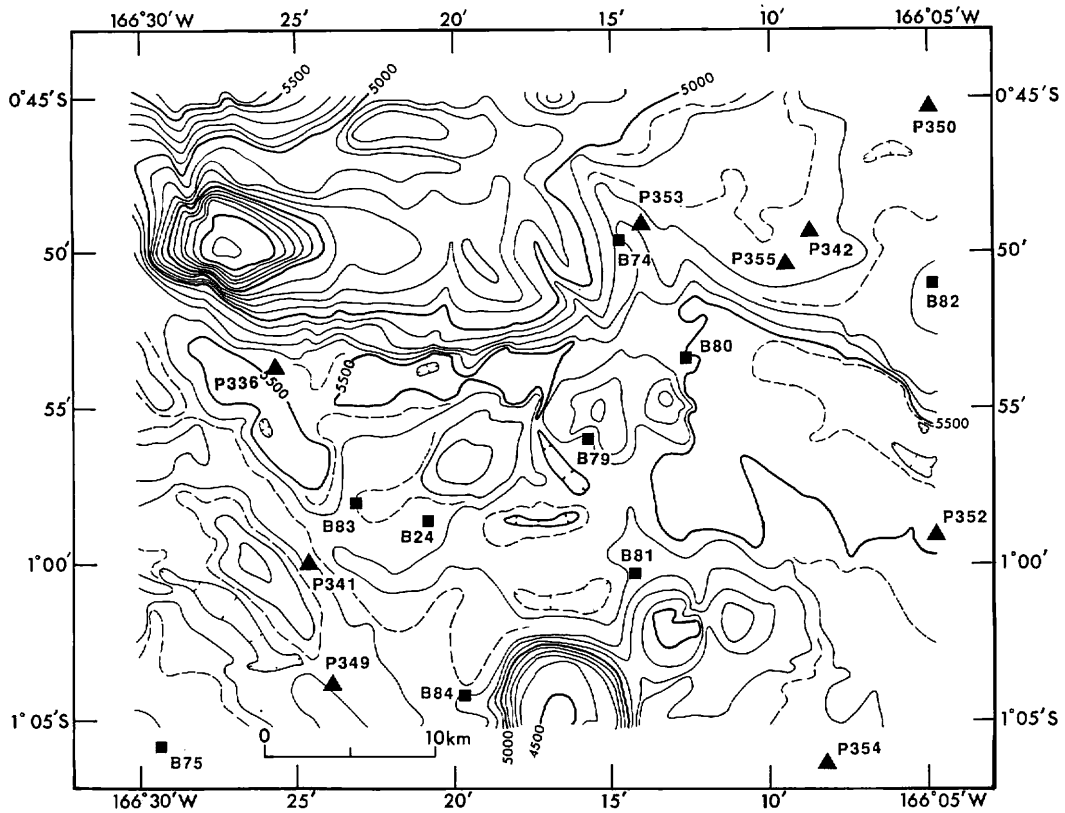

Fig. VI-2 Topography and sampling stations of the detailed survey area.

Table VI-1 Station data of box core during the GH82-4 Cruise.

Station No.	Sample No.	Position		water depth
		Latitude(S)	Longitude(W)	(m)
St. 3250	B70	0°43.74'	166°50.91'	4878
St. 3253	B71	0°41.03'	167°09.31'	3595
St. 3271	B72	1°59.34'	167°42.89'	5693
St. 3283	B73	2°28.22'	168°01.81'	5387
St. 3300	B74	0°49.62'	166°14.73'	5300
St. 3324	B75	1°05.86'	166°29.37'	5167
St. 3327	B76	1°29.60'	167°18.53'	5765
St. 3330	B77	1°08.26'	166°44.45'	5367
St. 3333	B78	1°18.51'	166°47.80'	5225
St. 3343	B79	0°55.96'	166°15.77'	5405
St. 3355	B80	0°53.25'	166°12.59'	5514
St. 3366	B81	1°00.31'	166°14.22'	5359
St. 3378	B82	0°50.89'	166°04.81'	5302
St. 3388	B83	0°58.10'	166°23.20'	5359
St. 3398	B84	1°04.22'	166°19.78'	5305

Table VI-2 Station data of piston core during GH82-4 Cruise.

Station No.	Sample No.	Position		water depth (m)
		Latitude(S)	Longitude(W)	
St. 3248	P336	0°53.36'	166°25.77'	5434
St. 3262	P337	1°32.97'	167°36.36'	5667
St. 3265	P338	1°47.70'	168°03.61'	5537
St. 3277	P339	1°40.52'	166°44.32'	5403
St. 3288	P340	1°52.67'	166°53.31'	5687
St. 3312	P341	1°00.05'	166°24.68'	5377
St. 3315	P342	0°49.18'	166°08.68'	5174
St. 3325	P343	1°54.65'	167°27.55'	5791
St. 3326	P344	1°43.48'	167°21.77'	5791
St. 3328	P345	1°22.65'	166°56.40'	5648
St. 3329	P346	1°11.87'	166°55.25'	5323
St. 3331	P347	1°14.37'	166°37.33'	5169
St. 3332	P348	1°10.83'	166°41.65'	5292
St. 3338	P349	1°03.94'	166°23.94'	5309
St. 3349	P350	0°45.17'	166°04.76'	5219
St. 3360	P351	1°10.01'	166°05.35'	5382
St. 3372	P352	0°59.05'	166°04.70'	5517
St. 3383	P353	0°49.07'	166°14.03'	5249
St. 3393	P354	1°06.33'	166°08.23'	5353
St. 3399	P355	0°50.34'	166°09.43'	5164

Table VI-3 Framework of sediment classification.

Pelagic clay *zeolite, siliceous fossil, calcareous fossil<5%*		
Zeolite rich clay *5%<zeolite<10%*	Siliceous fossil rich clay *5%<siliceous fossil<10%*	Calcareous fossil rich clay *5%<calcareous fossil<10%*
Zeolitic clay *10%<zeolite*	Siliceous clay *10%<siliceous fossil<30%*	Calcareous clay *10%<calcareous fossil<30%*
	Siliceous ooze *30%<siliceous fossil*	Calcareous ooze *30%<calcareous fossil*

1982). In several box core samples, foraminiferal tests are distinctly scattered at several tens cm below the sediment surface, which suggests that CCD lowered in the past.

The box core B78 shows presence of hiatus at 20 cm below the sea floor. Early Miocene siliceous ooze below the hiatus includes a plenty of reworked Eocene radiolarians (Fig. VI-3).

Core sequences in the survey area

This section describes core sequences in the survey area except for the detailed survey area (Fig. VI-4).

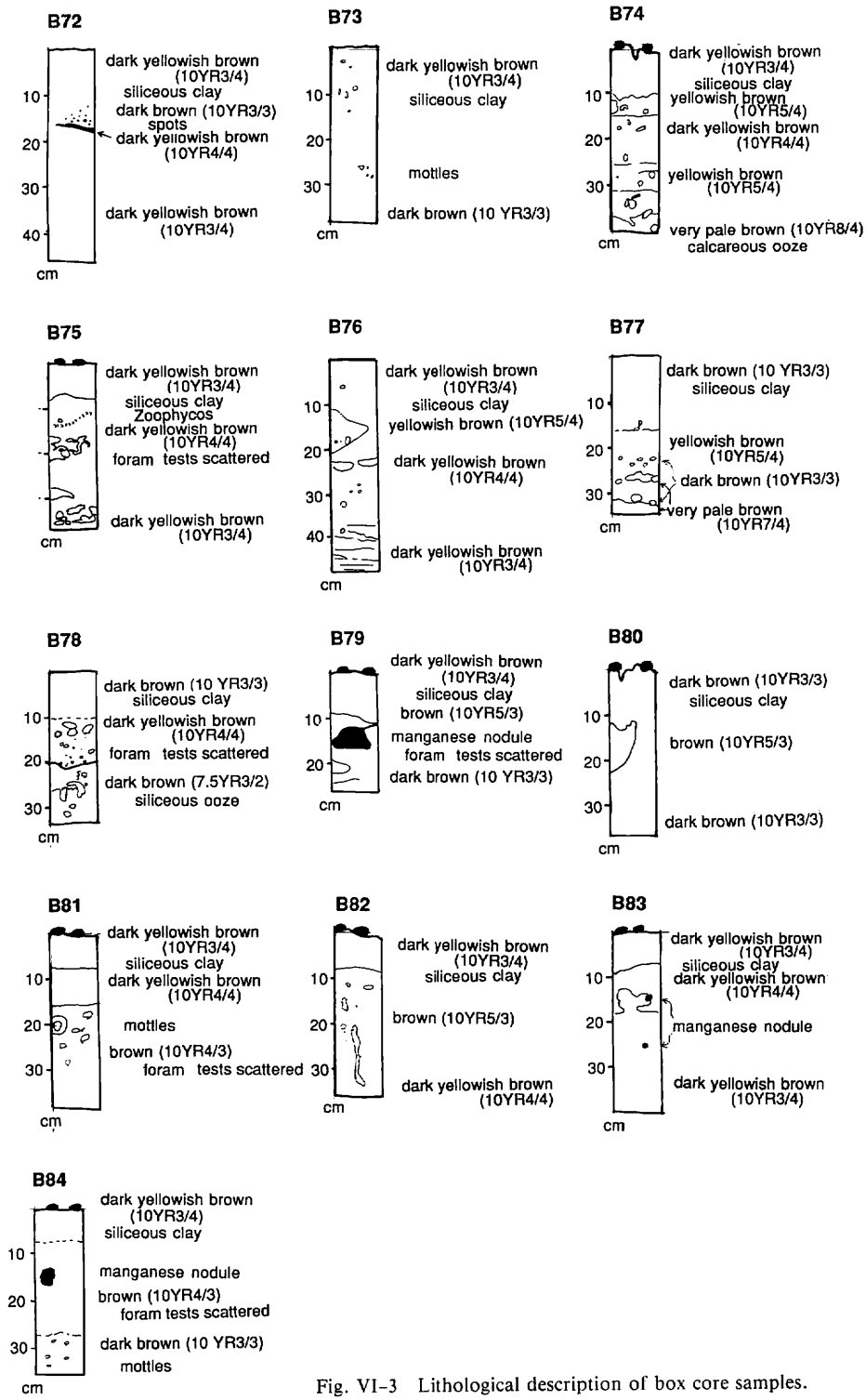

Fig. VI-3 Lithological description of box core samples.

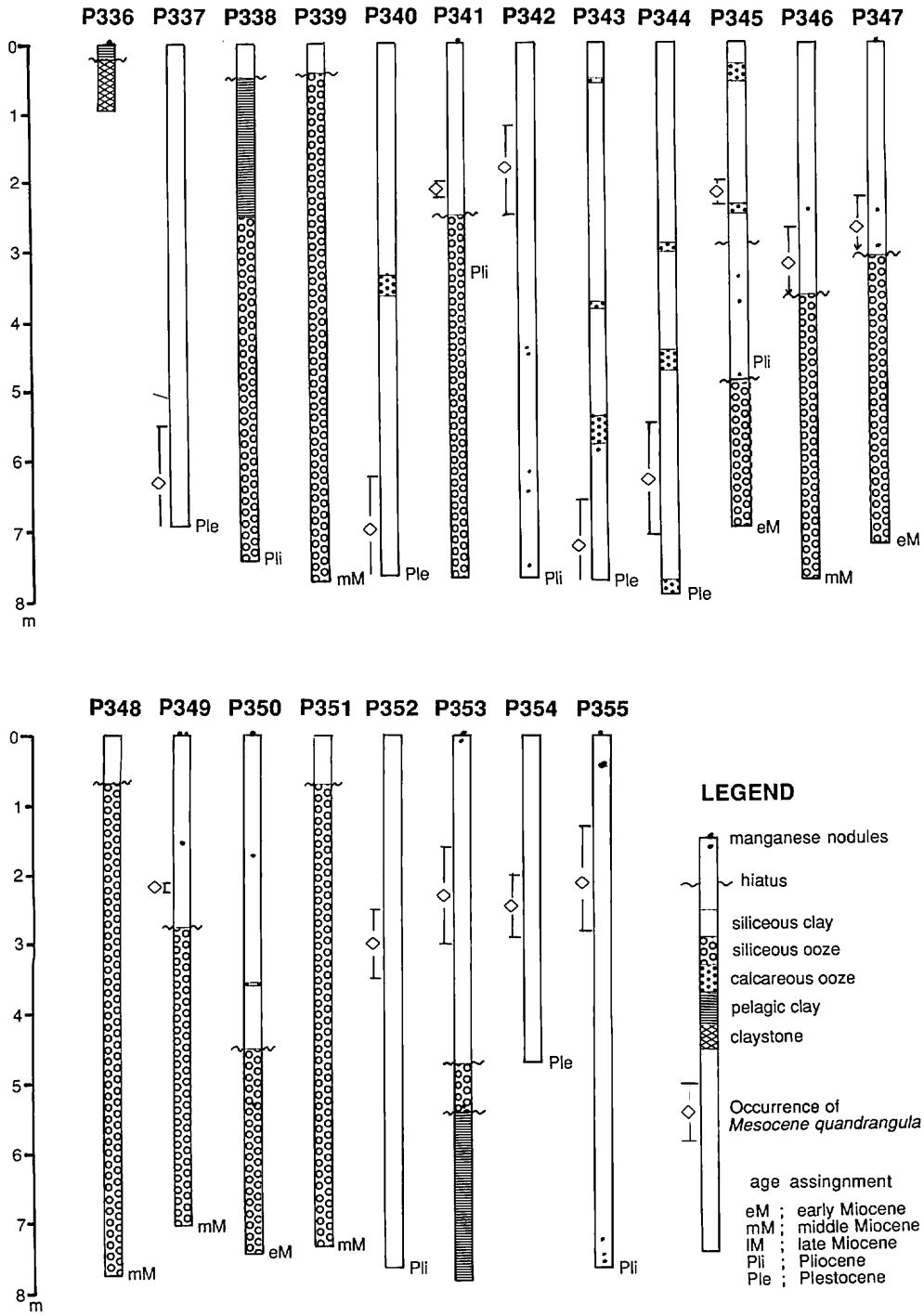

Fig. VI-4 Summarized core sequences collected during the GH82-4 Cruise.

Core P337: This core is composed of homogeneous dark brown siliceous clay with mottled structure. This core shows a continuous sedimentation since the early Pleistocene.
Core P338: This core has a hiatus at 50 cm from the core top. This core is composed of dark brown to dark yellowish brown siliceous clay in the uppermost, dark yellowish brown pelagic clay of the upper part, and dark brown to dark yellowish brown siliceous ooze in the middle to lower part of the core. The age below the hiatus is the latest Pliocene based on magnetostratigraphy (Yamazaki, Chapter VII, this volume).
Core P339: This core has a hiatus at 50 cm from the core top. This core is composed of dark yellowish brown siliceous ooze except dark brown siliceous clay of the uppermost ca. 50 cm. The age of siliceous ooze below the hiatus is the middle Miocene.
Core P340: This core is composed of dark yellowish brown siliceous clay throughout core sequence with one distinct layer of white to very pale brown calcareous ooze with ca. 30 cm thick at ca. 3.5 m from the core top. The calcareous layer is a turbidite with graded structure.
Core P343: This core is composed of siliceous clay throughout core sequence with three layers of light gray to yellowish brown calcareous ooze. These layers are turbidites.
Core P344: The lithology of this core is similar to that of Core P343. Very pale brown to light yellowish brown calcareous ooze are present at three horizons.
Core P345: Two hiatuses are suggested in this core sequence based on the magnetostratigraphic works at 290 cm and 480 cm from the core top. This core is composed of dark yellowish brown siliceous clay in the upper to middle part of the core and dark yellowish brown siliceous ooze of the lower part. The siliceous clay part has two layers of yellowish brown calcareous ooze. The age of the sediments between the two hiatuses is the Pliocene (late Gilbert Epoch–early Gauss Epoch) and the age of the sediments below the lower hiatus is the early Miocene.
Core P346: This core is composed of dark yellowish brown siliceous clay in the upper half and dark yellowish brown siliceous ooze of the lower half of the core. The lithologic change at 360 cm corresponds to a hiatus and the age of the sediments below the hiatus is the middle Miocene.
Core P347: This core is composed of yellowish brown to dark yellowish brown siliceous clay in the upper half and dark yellowish brown siliceous ooze of the lower half of the core. The core sequence is similar to that of Core P 346.
Core P348: This core is composed of dark yellowish brown siliceous ooze except dark brown siliceous clay of the upper ca. 70 cm. The age of siliceous ooze is the middle Miocene. One thin calcareous ooze layer is intercalated in the siliceous clay in the pilot core.

The average sedimentation rates in the Quaternary based on the magnetostratigraphy are 6–9 mm/ky for the sediment cores with turbidite layers and 2–3 mm/ky for the sediment cores without turbidites.

Core sequences in the detailed survey area

In the detailed survey area, ten piston cores were sampled at short intervals (Fig. VI-4)

Core P336: This core is only 90 cm long because of its poor penetration. This core is composed of unconsolidated pelagic clay of the uppermost 30 cm and semi-consolidated brown to pale yellow claystone. The claystone in the core catcher yields conical *Dictyomitra*-type radiolarian molds, suggesting the Cretaceous age.
Core P341: This core is composed of dark yellowish brown siliceous clay of the upper part and dark yellowish brown siliceous ooze of the lower part of the core. The lithologic change at 270 cm corresponds to a hiatus and the age of the sediments below the hiatus is the early Pliocene.
Core P342: This core is composed of dark yellowish brown siliceous clay throughout the core. Magnetostratigraphy shows continuous slow sedimentation back to 3.5 Ma.
Core P349: This core has a hiatus at 275 cm from the core top. This core is composed of dark yellowish brown to dark brown siliceous clay of the upper part and dark yellowish brown siliceous ooze of the lower part of the core. The age of the sediments below the hiatus is the middle Miocene.
Core P350: This core has a hiatus at 450 cm from the core top. This core is composed of yellowish brown to brown dark yellowish brown siliceous clay of the upper part and siliceous ooze of the lower part of the core. The age of the sediments below the hiatus is the early Miocene.
Core P351: The uppermost 30 cm of this core is composed of dark brown siliceous clay and the rest of dark yellowish brown siliceous ooze . The age of the core catcher is the middle Miocene.
Core P352: This core is composed of dark yellowish brown siliceous clay throughout the core. This core shows continuous sedimentation since the late Pliocene.
Core P353: This core has two hiatus at 470 cm and 560 cm from the core top. This core is composed of dark yellowish brown siliceous clay in the upper part, dark yellowish brown siliceous ooze in the middle part and the rest of very dark brown pelagic clay. The age of the sediments below the lower hiatus is unknown because of absence of siliceous and calcareous microfossils in the sediments.
Core P354: This core is short because 4-m long core barrel was used for coring. This core is composed of dark brown to dark yellowish brown siliceous clay throughout the core. The core shows a continuous sedimentation since the early Pleistocene.
Core P355: This core is composed of siliceous clay throughout the core. This core shows a continuous sedimentation since the late Pliocene.

The average sedimentation rates in the Quaternary calculated based on the magnetostratigraphy range between 1.0 and 3.3 mm/ky except for the Core P350 (>5.8 mm/ky). These sedimentation rates are smaller than those of the whole GH82-4 area and similar to those of the previous survey areas (GH80-5 and GH81-4 areas) of Geological Survey of Japan north of the equator (Nishimura, 1986).

Hiatuses in the core sequences

Half of the core sequences studied show the stratigraphic breaks, hiatuses. Antarctic Bottom Water (AABW) flows into the Central Pacific Basin through the Samoan Passage (Hollister *et al.*, 1974) and a part of AABW flows eastward along the Nova-Canton Trough in the survey area (Yamazaki, chapter V of this volume). The hiatuses were probably formed when AABW was intensified enough to erode sediments and/or

to prevent sedimentation. The short periods of hiatus have been recognized and numbered based on DSDP core data (Keller and Barron, 1987). In GH82-4 area, only the period of the uppermost hiatus in the core sequences is cleared. The peak of the erosion is probably a period between the Olduvai Event and the Jaramillo Event in the Matuyama Reversed Epoch.

Calcareous biogenic turbidite

In the survey area, Cores P340, P343, P344, and P345 include the layers of calcareous ooze of several tens cm thick showing upward grading (Fig. VI-4). The lithology and sedimentary structure suggest that these layers are turbidites. Biogenic carbonate turbidites have been reported in the other areas of the Central Pacific Basin, (Nishimura *et al.*, 1986). These turbidites are derived from the topographic highs near the turbidite distribution area. The age of the turbidite sedimentation is cleared by the micropaleontology and magnetostratigraphy. The frequency of the turbidites are 3 to 4 times per million year, which is very small compared with that of turbidites in and around the oceans of active margins.

The seismic records of air gun show a wide and complicated distribution of turbidite facies (Tanahashi, chapter IV of this volume). The distribution of turbidite is highly affected by topography and shows complicated drainage pattern and buries basin floors like channeled turbidites in the southwest of the Line Island Archipelago (Orwig, 1987). Source of the biogenic turbidites is probably the Manihiki Plateau to the south of the survey area, on which calcareous ooze are dominated above CCD (Nakao and Mizuno, 1982). The turbidite sedimentation may prevent formation of manganese nodules because of the cessation of the upward lifting of nodules due to immediate burial of nodules.

Micropaleontology

Core-bottom sediment samples and some additional ones were micropaleontologically analyzed for age estimation of the core sequences.

Silicoflagellates

The occurrence of easily distinguished silicoflagellates species *Mesocene quandrangula* Ehrenberg were determined on smear slides. This species has a short acme around the Jaramillo Event of the Matuyama Reversed Epoch (Zhuze and Mukhina, 1973) and dated from 0.79 to 1.3 Ma (Berggren *et al*, 1980). The acme of this species is distinct and the peak of the abundance of this species exceeds 80% of total silicoflagellate flora (Nishimura, 1986). The observed horizons of this species are shown in Figure VI-4.

Radiolarians

The radiolarian biostratigraphy of the tropical region were established back to the Eocene (Riedel and Sanfilippo, 1978). The relation between the radiolarian datum and magnetostratigraphic time scale were also established (Theyer *et al.*, 1978). Preliminary works of the radiolarian species were carried out on the core catcher samples of the piston cores in this area. Additional samples were selected for the

Table VI-4 Occurrence of radiolarians of piston core samples.

Sample	Species	Age
P336	*Dictyomitra*-type radiolarian inner molds	Cretaceous?
P337	*Spongaster tetras* Ehrenberg	< 3.4 Ma
	Ommatartus tetrathalamus (Haeckel)	
	Amphirhopalum ypsilon Haeckel	
	Lithopera bacca Ehrenberg	
P338 CC	*Pterocanium prismatium* Riedel	5-4 Ma
	Stichocorys peregrina (Riedel)	
	Solenosphaera omnitubus Riedel and Sanfilippo	
	Lithopera bacca Ehrenberg	
	Ommatartus penultimus (Riedel)	
P339 CC	*Cannartus tubarius* Haeckel	ca. 11 Ma
	Cannartus laticonus Riedel	
	Ommatartus hughesi (Campel and Clark)	
	Dictyocoryne ontongensis Riedel and Sanfilippo	
	Lithopera bacca Ehrenberg	
P340 CC	*Ommatartus penultimus* (Riedel)	< 3.4 Ma
	Spongaster tetras Ehrenberg	
P341 IV20	*Spongaster tetras* Ehrenberg	3.4-3.6 Ma
	Spongaster pentas Riedel and Sanfilippo	
	Solenosphaera omnitubus Riedel and Sanfilippo	
P341 CC	*Lithopera thornburgi* Riedel and Sanfilippo	
P342 CC	*Solenosphaera omnitubus* Riedel and Sanfilippo	4.3 Ma<?
	Ommatartus penultimus (Riedel)	
	Canartus violina Haeckel	
	Dorcadospyris dentata Haeckel	
P343 CC	*Ommatartus tetrathalamus* (Haeckel)	<3.8Ma
P345 VI20	*Spongaster tetras* Ehrenberg	3.4-3.6 Ma
	Spongaster pentas Riedel and Sanfilippo	
	Pterocanium prismatium Riedel	
P345 CC	*Canartus violina* Haeckel	17.5-15.5 Ma
	Dorcadospyris dentata Haeckel	
	Cyrtocapsella tetrapera Haeckel	
	Lychnocanoma elongata (Vinassa)	
P346 CC	*Cannartus laticonus* Riedel	13.5-11 Ma
	Lychnocanoma elongata (Vinassa)	
	Dorcadospyris atlaa Haeckel	
P347 CC	*Cyrtocapsella tetrapera* Haeckel	17.5-15.5 Ma
	Dorcadospyris dentata Haeckel	
	Canartus violina Haeckel	
P348 CC	*Lychnocanoma elongata* (Vinassa)	ca. 11 Ma
	Dictyocoryne ontongensis Riedel and Sanfilippo	
	Lithopera thornburgi Riedel and Sanfilippo	
	Canartus petterssoni Riedel and Sanfilippo	
	Cannartus laticonus Riedel	
	Ommatartus antepenultimus Riedel and Sanfilippo	
	Dorcadospyris dentata Haeckel	
P349 CC	*Cyrtocapsella tetrapera* Haeckel	13.5-11.4 Ma
	Cannartus laticonus Riedel	
	Canartus petterssoni Riedel and Sanfilippo	
	Dorcadospyris alata (Riedel)	
	Lithopera thornburgi Riedel and Sanfilippo	
P350 CC	*Cannartus prismaticus* (Haeckel)	24.2-17.2 Ma
	Lychnocanoma elongata (Vinassa)	
P351 CC	*Dorcadospyris alata* (Riedel)	11.1-14.2 Ma
	Dorcadospyris dentata Haeckel	
	Cyrtocapsella tetrapera Haeckel	
	Lychnocanoma elongata (Vinassa)	
	Canartus violina Haeckel	
P352 CC	*Spongaster tetras* Ehrenberg	<3.4 Ma
	Spongaster pentas Riedel and Sanfilippo	
	Pterocanium prismatium Riedel	
P353 CC	no radiolarian	
P354 CC	*Pterocanium prismatium* Riedel	<3.4 Ma
	Ommatartus hughesi (Campel and Clark)	
	Spongaster tetras Ehrenberg	
	Cannartus mammifer (Haeckel)	
P355 CC	*Spongaster pentas* Riedel and Sanfilippo	3.4-4.6 Ma
	Stichocorys peregrina (Riedel)	
	Pterocanium prismatium Riedel	
	Ommatartus tetrathalamus (HAeckel)	
	Ommatartus penultimus (Riedel)	
	Ommatartus hughesi (Campel and Clark)	

recognition of magnetostratigraphy of the core sequences. The results are shown in Table V-4 and some results are already quoted in the earlier sections.

Summary

1) Surface sediments of this area are dark brown siliceous clay with high contents of radiolarian and diatom tests, because of high productivity and depth below CCD.
2) The succession of the core sequences is divided into two lithologic units, that is, siliceous ooze of the Miocene age and siliceous clay of the Pliocene to the Pleistocene age. Locally pelagic clay was deposited in the Pliocene age.
3) Sedimentation rates of this area in the Quaternary are not so rapid even in an equatorial high productivity zone. The rates are similar to those of the previous survey areas of GSJ north of the equator, where manganese nodules were abundant.
4) The core sequences suggest hiatuses with valuable term since the middle Miocene to the early Quaternary. The period of the uppermost hiatus is from the late Pliocene to the early Pleistocene. These hiatuses were probably formed under the influence of intensified AABW.
5) Several core sequences have calcareous biogenic turbidites probably derived from the Manihiki Plateau to the south of the survey area.

References

Berger, W. H., Adelseck, C. G. and Mayer, L. A. (1976) Distribution of carbonate in surface sediments of the Pacific Ocean. *Jour. Geophys. Res.*, vol. 81, p. 2617–1627.

Berggren, W. A., Burckle, L. H., Cita, M. B., Cooke, H. B. S., Funnell, M. B., Cartner, S., Hays, J. D., Kennett, J. P., Opdyke, N. D., Pastouret, L., Shackleton, N. J. and Takayanagi, Y. (1980) Towards a quaternary Time scale. *Quaternary Research*, vol. 13, p. 277–302.

Hollister, C. D., Johnson, S. A. and Lonsdale, P. F. (1974) Current-controlled abyssal sedimentation: Samoan Passage, equatorial Pacific. *Journal of Geology*, vol. 82, p. 275–300.

Keller, G. and Barron, J. A. (1987) Paleodepth distribution of Neogene deep-sea hiatuses. *Paleoceanography*, vol. 2, p. 697–713.

Lineberger, P. H. (1975) Sedimentary processes and pelagic turbidites in the eastern Central Pacific Basin. *Hawaii Inst. Geophys. Rep.*, HIG-75-24, 115 p.

Nakao, S. and Mizuno, A. (1982) Regional sedimentologic data: the Central Pacific Wake-Tahiti transect, GH80-1 Cruise. *Geol. Surv. Japan Cruise Rept.*, no. 18, p. 95–123.

Nishimura, A. (1984) Deep-sea sediments in the GH80-5 area in the northern vicinity of the Magellan Trough. *Geol. Surv. Japan Cruise Rept.*, no. 20, p. 67–89.

——— (1986) Deep-sea sediments in the Central Equatorial Pacific (GH81-4 area). *Geol. Surv. Japan Cruise Rept.*, no. 21, p. 56–83.

———, Yamazaki, T., Ikehara, K. and Tanahashi, M. (1987) Calcareous biogenic turbidites in the Central Pacific Basin. *Jour. Sedimentol. Soc. Japan*, no. 22/23, p. 65–70.

Orwig, T. (1981) Channeled turbidites in the eastern Central Pacific Basin. *Marine Geol.*, vol. 39, p. 33–57.

Piper, D. Z., Macoy, E. W., Swint, T. R. *et al.* (1985) *Manganese nodules, seafloor sediment, and sedimentation rates of the Circum-Pacific Region*. American Association of Petroleum Geologists, Tulsa, Oklahoma, scale 1:17,000,000.

Riedel, W. R. and Sanfilippo, A. (1978) Stratigraphy and evolution of tropical Cenozoic radiolarians. *Micropaleontology*, vol. 23, p. 61–96.

Takayanagi, Y., Sakai, T., Oda, M. and Hasegawa, S. (1982) Micropaleontology of piston cores, Wake to Tahiti. *Geol. Surv. Japan Cruise Rept.*, no. 18, p. 238–263.

Theyer, F., Mato, C. Y. and Hammond, S. R. (1978) Paleomagnetic and geochronologic calibration of latest Oligocene to Pliocene radiolarian events, Equatorial Pacific. *Marine Micropaleont.*, vol. 3, p. 377–395.

Winterer, E., L., Ewing, J. L. *et al.* (1973) *Initial Rept. Deep Sea Drilling Project, 17.* U. S. Government Printing Office, Washington D. C., 930 p.

Zhuze, A. P. and Mukhina, V. V. (1973) The Mesocena elliptica Ehr. zone in the Pleistocene sediments of the Pacific Ocean. *Oceanology*, vol. 13, p. 386–394.